Electrogenicity accompanies photoreduction of the iron-sulfur clusters F_A and F_B in photosystem I

Mahir D. Mamedov[a], Kira N. Gourovskaya[a], Ilya R. Vassiliev[1,b], John H. Golbeck[b], Alexey Yu. Semenov[a,*]

[a] *Department of Photobiochemistry, A.N. Belozersky Institute of Physico-Chemical Biology, Moscow State University, 119899 Moscow, Russia*
[b] *Department of Biochemistry and Molecular Biology, The Pennsylvania State University, S-310 Frear Laboratory, University Park, PA 16802-4500, USA*

Received 2 June 1998

Abstract Photovoltage responses accompanying electron transfer on the acceptor side of photosystem I (PS I) were investigated in proteoliposomes containing PS I complexes from the cyanobacterium *Synechococcus* sp. PCC 6301 using a direct electrometrical technique. The relative contributions of the $F_X \rightarrow F_B$ and the $F_X \rightarrow F_A$ electron transfer reactions to the overall electrogenicity were elucidated by comparing the sodium dithionite-induced decrease in the magnitude of the total photoelectric responses in control and in F_B-less ($HgCl_2$-treated) PS I complexes. The results obtained suggest that the electrogenesis on the acceptor side of PS I is related to electron transfers between both F_X and F_A and F_A and F_B. Based on the electrogenic nature of the latter reaction in PS I complexes, we conclude that F_A rather than F_B is the acceptor proximal to F_X.

Key words: Proteoliposome; Photosystem I; Photoelectric response; Electrogenicity; *Synechococcus sp.* PCC 6301

1. Introduction

Photosystem I (PS I) catalyzes the reduction of soluble ferredoxin or flavodoxin and the oxidation of plastocyanin or cytochrome c_6 by a multi-step electron transfer process initiated by light. The initial step involves charge separation between the primary donor P700, a chlorophyll *a* dimer, and the primary acceptor A_0, a chlorophyll *a* monomer. This step is followed by subsequent electron transfer through A_1 (phylloquinone), and three iron-sulfur clusters, F_X, F_A and F_B. P700, A_0, A_1 and F_X are bound to the PsaA/PsaB heterodimer, while F_A and F_B are located on the stromal PsaC subunit. The kinetics of forward electron transfer from P700 to A_0 takes place in a few picoseconds and further electron transfer to A_1 takes place in times shorter than 50 ps. The electron is then transferred from A_1 to F_X and in the following step to F_A/F_B in the submicrosecond time range. One of the most challenging questions regarding the arrangement of the electron cofactors within the PS I complex concerns the sequence of electron transfer between the two terminal iron-sulfur clusters, F_A and F_B (for discussion see [1]). One promising strategy used to approach the acceptor sequence problem involves chemical extraction of one of the clusters, F_B [2–6]. Our recent results based on single-turnover laser flash excitation to promote step-by-step electron transfer in control and F_B-less PS I complexes in the presence of the efficient electron donor for $P700^+$, phenazine methosulfate, also argue for the assignment of F_B as the F_X-distal cluster [5]. The same conclusion was reached by analysis of the reduction kinetics of ferredoxin externally added to control and F_B-less PS I complexes [6].

Electron transfer from P700 to the terminal iron-sulfur clusters F_A/F_B is electrogenic [7–10]. Given that the vector between the two terminal clusters is tilted from the membrane normal [11], electrogenicity developed from electron transfer between these clusters is expected. However, the relative magnitudes of the electrogenic steps accompanying electron transfer between F_X and F_A, and between F_A and F_B are not yet estimated. The goal of the present work is to investigate the photovoltage changes due to electron transfer between the clusters F_X, F_A and F_B in control and in F_B-less ($HgCl_2$-treated) PS I complexes. We use this information in an attempt to provide insight into the sequence of electron transfer between the terminal acceptors F_A and F_B.

2. Materials and methods

Soybean lecithin (type IIS), Tris, sodium cholate, 2,6-dichlorophenol-indophenol (DCPIP), sodium ascorbate, sodium dithionite, potassium ferricyanide, $CaCl_2$ and Sephadex G-50 were purchased from Sigma (St. Louis, MO, USA). Other reagents were commercial products of the highest purity available. PS I complexes were prepared from *Synechococcus* sp. PCC 6301 as described in [12], and extraction of the F_B cluster followed the protocol described in [4]. Proteoliposomes with PS I complexes were prepared as described in [13]. Transmembrane electric potential difference ($\Delta\Psi$) measurements in PS I-containing proteoliposomes were performed in anaerobic conditions as described in [9]. The instrument rise time was 200 ns. Saturating light flashes were provided by a frequency doubled Quantel Nd:YAG laser (λ= 532 nm; pulse half-width, 15 ns; flash energy, 40 mJ). Multiexponential analysis of the photoelectric response kinetics was performed using Igor Pro v. 3.11 (Wavemetrics, Inc., Lake Oswego, OR, USA).

3. Results

Flash excitation of PS I complexes incorporated into liposomes adsorbed on the surface of a phospholipid-impregnated collodion film leads to a $\Delta\Psi$ formation corresponding to the negative charging of the interior of the proteoliposomes (Fig. 1). The $\Delta\Psi$ amplitude is proportional to the sum of the dielectrically weighted distances between the electron carriers in the PS I complex. Although $\Delta\Psi$ is developed within a time shorter than the instrument-limited response time constant of 200 ns, the initial amplitude of $\Delta\Psi$ can be determined based on extrapolation of the $\Delta\Psi$ decay kinetics. The main decay

*Corresponding author. Fax: (7) (095) 939-0338.
E-mail: semenov@electro.genebee.msu.su

[1] On leave from Department of Biophysics, Faculty of Biology, Moscow State University, 119899 Moscow, Russia.

PII: S0014-5793(98)00759-5

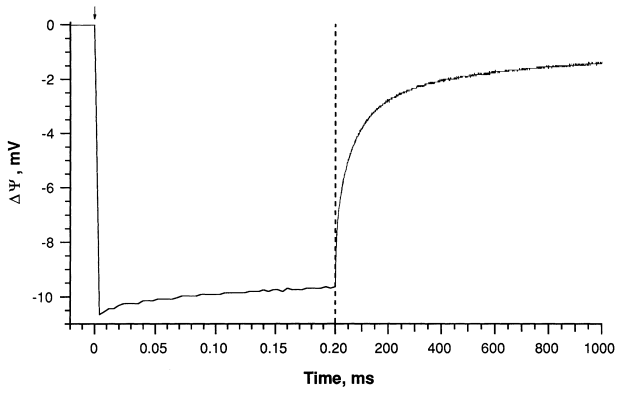

Fig. 1. Representative flash-induced photoelectric response in proteoliposomes containing PS I complexes from *Synechococcus* sp. PCC 6301. Incubation medium contains 200 mM glycine buffer, pH 10, 10 mM sodium ascorbate and 4 μM DCPIP. The oxygen contained in the buffer solution was substituted by high-purity argon gas.

pathway of the ΔΨ built across the membrane is the charge recombination between $P700^+$ and the photoreduced terminal acceptor, but in a fraction of complexes this pathway may be substituted by a slower passive discharge. This may occur as a result of the interaction of $P700^+$ with an artificial donor or due to oxidation of the terminal acceptor (for instance, by a trace amount of oxygen present in the medium).

Taking into account that F_B can be selectively extracted by $HgCl_2$ treatment, we consider two possible sequences of the iron-sulfur clusters: F_A is proximal to F_X and F_B is proximal to F_X. (1) If F_A is the terminal cluster, the amplitude of the electrogenic response should be the same for the control and $HgCl_2$-treated samples. Under these conditions, we assume that F_A is capable of photoreduction in the absence of F_B. (2) If F_B is the terminal cluster, the amplitude of the electrogenic response should be lower in the $HgCl_2$-treated sample. The ability of F_A to be reduced in either instance follows from the tens of milliseconds decay kinetics of $P700^+$ reduction in $HgCl_2$-treated PS I complexes [5,14]. The amplitudes of the photoelectric responses can be compared for different samples only if the number of PS I complexes per unit membrane surface is constant between the PS I samples. This is a difficult condition to meet in the estimation of a relatively small amplitude change. To overcome this limitation, we normalized the ΔΨ amplitudes corresponding to the intrinsic charge recombination in the PS I complexes by using the ΔΨ amplitudes obtained after chemical reduction of the PsaC-bound cluster(s), F_A and F_B. Based on the room temperature kinetics of P700 absorbance change, the amount of dithionite used (100 mM) was found to be sufficient to chemically reduce F_A and F_B without any apparent reduction of F_X in the isolated PS I complexes (not shown). Thus, all ΔΨ amplitudes are normalized to the dithionite-independent amplitude of the P700 to F_X charge separation.

In the presence of a slow electron donor, DCPIP, the kinetics of ΔΨ decay can be decomposed into five exponents with lifetimes (τ) of 7.9 μs, 415 μs, 3.5 ms, 31 ms, 138 ms and 924 ms (Fig. 2, left). Components with τ values of 31 ms (21.3% of amplitude) and 138 ms (31.5%) correspond to the charge recombination between $P700^+$ and $(F_A/F_B)^-$, while the 924 ms component (20.2%) corresponds to a passive discharge across the membrane. The minor components with τ = 415 μs and 3.5 ms correspond to back reactions from F_X^- in a fraction of centers with impaired forward electron transfer to F_A and F_B. The lifetime values derived from the photovoltage measurements are in good agreement with optical spectroscopic measurements of the kinetics of $P700^+$ reduction in the near IR [5,14]. The fast decay phases with the lifetimes of ca. 5–10 μs and 70–200 μs and variable amplitudes could be observed in most of measurements. Although these lifetimes correspond to the lifetimes of A_1^- back-derived from optical data [14,15], we cannot rigorously exclude that the 5–10 μs decay phase is related to some electrical artifact [14]. To determine the initial amplitude of ΔΨ we took into account only those charge separation components with lifetimes longer than 400 μs, i.e. those related to electron transfer at distances greater than that between P700 and A_1. This excluded contributions from centers with impaired electron transfer between A_1 and F_X and the possible above mentioned electrical artifact. Addition of 100 mM dithionite to the electrometric cell compartment containing one and the same sample leads to the expected acceleration of the ΔΨ decay kinetics, which now is due to the backreaction of F_X^-. Multi-exponential analysis of the kinetics yield components with lifetimes of 11 μs, 97 μs, 963 μs, 5.1 ms and 18 ms and relative contributions of 13.6, 8, 22, 46.1 and 10.3%, respectively.

The deconvolution shows a decrease in the amplitude of the photoelectric response in the presence of dithionite, which occurs due to blockage of electron transfer between F_X and F_A/F_B (Fig. 2, left). This alone indicates that electron transfer between the iron-sulfur clusters F_X and F_A/F_B is electrogenic. Although the time constant of our experimental setup did not allow measurement of the forward kinetics of electron transfer between F_X and F_A/F_B, our data is consistent with electron transfer occurring between the iron-sulfur centers in PS I in the submicrosecond time range.

Treatment of cyanobacterial PS I complexes with $HgCl_2$ results in >95% destruction of the F_B iron-sulfur cluster and in the retention of >90% of the F_A [5]. For the $HgCl_2$-treated samples we performed identical multi-exponen-

Table 1
Calculation of the F_X-F_B region dielectric constant

Sample	Membrane potential ratio Ψ_{XB}/Ψ_{PX}	Average Ψ_{XB}/Ψ_{PX}	Distance ratio D_{XB}/D_{PX}	Dielectric constant ratio $\varepsilon_{XB}/\varepsilon_{PX}$
1	0.41			
2	0.39	0.41 ± 0.03	0.61	1.47
3	0.44			

The ratio between the dielectric constants corresponding to electron transfer from F_X to F_B and from P700 to F_X ($\varepsilon_{XB}/\varepsilon_{PX}$) is related to the photovoltages dropped between F_X and F_B (Ψ_{XB}) and between P700 and F_X (Ψ_{PX}) by the equation: $\varepsilon_{XB}/\varepsilon_{PX} = (D_{XB}/D_{PX}):(1/L_{XA} \times L_{AB}+1):(\Psi_{XB}/\Psi_{PX}) = 0.61:1.01:0.41 = 1.47$, where D_{XB} and D_{PX} are the projections for the $F_X \rightarrow F_B$ and $P700 \rightarrow F_X$ distance vectors to the membrane normal, respectively; $L_{XA} = 70$ and $L_{AB} = 1.15$ are the microscopic equilibrium constants between F_X and F_A and between F_A and F_B, respectively (see Section 4 for details).

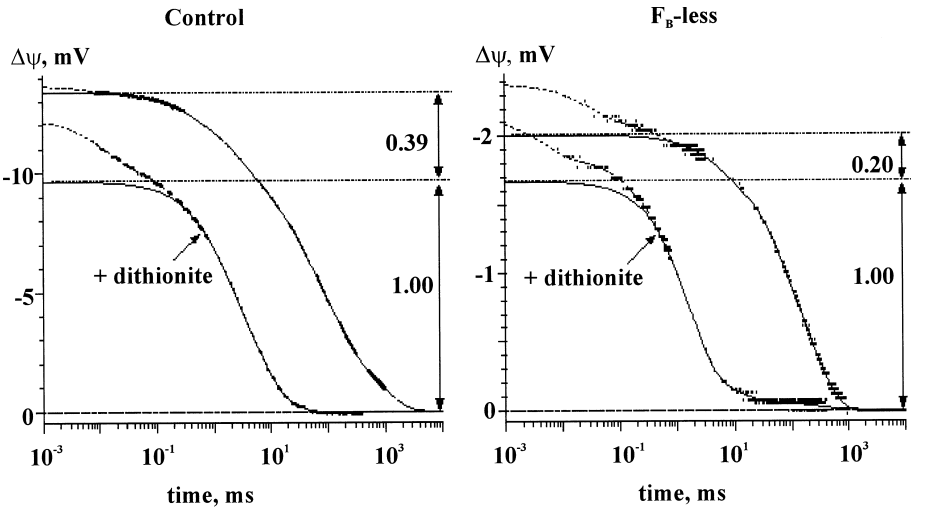

Fig. 2. Decay kinetics of the flash-induced photoelectric responses in proteoliposomes containing control and F_B-less PS I complexes in the absence (top curves) and in the presence of 100 mM sodium dithionite. The pH value after incubation in the presence of dithionite was controlled before registration. Experimental conditions as in Fig. 1. Dashed curves indicate the multiexponential data fits; solid lines are fit curves with the fast components ($\tau < 400$ μs) being subtracted. Horizontal lines indicate the initial amplitudes of the photoelectric responses. The kinetics are normalized to the initial amplitudes obtained after subtraction of the fast (< 400 μs) components.

tial analysis of the kinetics in the absence and in the presence of dithionite and determined the initial amplitudes of ΔΨ after subtracting the fast phases with the lifetimes shorter than 400 μs (Fig. 2, right). In the absence of dithionite the major components have lifetimes of 4.8 ms (10.6%), 71.4 ms (31%) and 292 ms (43.7%), while addition of dithionite leads to a faster kinetics with major components of 1.6 ms (65.2%) and 10.6 ms (10.1%). It is evident that addition of dithionite to both control (Fig. 2, left) and Hg-treated (Fig. 2, right) PS I complexes results in a similar acceleration of the ΔΨ kinetics, but in the latter case the decrease of the initial ΔΨ amplitude was less significant. Although the absolute ΔΨ amplitudes varied between different samples (not shown), the more pronounced effect of dithionite on the initial amplitude in the control samples was consistently observed (see Tables 1 and 2).

4. Discussion

Although the F_A and F_B clusters were among the first acceptors to be discovered in PS I, the issue of the sequence of electron transfer among them is still controversial. Although time-resolved optical spectroscopy can in principle resolve the rise times of the acceptors, the difference spectra of F_A, F_B and F_X are nearly identical, with a broad and relatively weak bleaching due to S→Fe charge transfer bands centered around 430 nm [15]. Conversely, F_A, F_B and F_X can be distinguished by low-temperature EPR spectroscopy, but the instrument response time is insufficient to determine rates of electron transfer between the iron-sulfur clusters. Thus application of photovoltage measurements, which are indicative of directionality of electron transport in membrane-oriented complexes, is a promising approach to resolve the sequence of electron transfer among the iron-sulfur clusters in PS I.

Photovoltage measurements have been applied in several laboratories in an attempt to resolve the forward electron transfer kinetics in PS I. Sigfridsson et al. [8] resolved several kinetic phases in the flash-induced ΔΨ increase of spinach PS I particles oriented in a phospholipid layer adsorbed on Teflon film. The kinetic phase with time constant of 30 μs was ascribed to electron transfer from F_B to F_A while the 200 μs phase was assigned to electron transfer out of PS I, a proton transfer in the opposite direction, or a conformational change. Leibl et al. [7] studied the flash-induced kinetics of ΔΨ generation of oriented PS I membranes from *Synechocystis* sp. PCC 6803 which formed a multilayer on a platinum electrode. Besides an unresolved rapidly rising phase, an additional positive electrogenic phase was observed with a time constant of 220 ns. Assuming that the reduction of F_X is the rate limiting process for the reduction of F_A/F_B, this phase can be attributed to electron transfer from A_1^- via F_X to F_A/F_B. It is likely that the different photovoltage kinetics reported by Leibl et al. [7] and by Sigfridsson et al. [8] reflect different capabilities of methods used in these laboratories. However, one cannot also exclude the possibility of differences between PS I complexes prepared from higher plants and cyanobacteria. Our experimental results are more compatible with those obtained by Leibl et al. [7] than by Sigfridsson et al. [8], since we did not observe any additional phases of ΔΨ increase in the microsecond time scale. A comparison of the dithionite-induced decrease of the magnitude of the total photoelectric

Table 2
Calculation of the F_X-F_A region dielectric constant

Sample	Membrane potential ratio Ψ_{XA}/Ψ_{PX}	Average Ψ_{XA}/Ψ_{PX}	Distance ratio D_{XA}/D_{PX}	Dielectric constant ratio $\varepsilon_{XA}/\varepsilon_{PX}$
1	0.2			
2	0.18	0.19 ± 0.01	0.42	2.19

The ratio between the dielectric constant values corresponding to electron transfer from F_X to F_A and from P700 to F_X yields the following equation: $\varepsilon_{XA}/\varepsilon_{PX} = (D_{XA}/D_{PX}):(1/L_{XA}+1):(\Psi_{XA}/\Psi_{PX}) = 0.42:1.01:0.19 = 2.19$, where D_{XA} is the projection for the $F_X \rightarrow F_A$ distance vector to the membrane normal; Ψ_{XA} is the photovoltage dropped between F_X and F_A.

responses obtained with control and $HgCl_2$-treated PS I complexes provides an independent approach for elucidation of the relative contribution of $F_X \rightarrow F_B$ and $F_X \rightarrow F_A$ electron transfer reactions to the overall electrogenesis within the PS I complex.

Given the close midpoint potentials of F_A and F_B as well as the high ($> 10^4$ s^{-1}) electron exchange rate between the clusters (as implied from broadening of ^1H NMR resonances of partially reduced clusters in unbound PsaC [16]), it is reasonable to assume that the $\Delta\Psi$ amplitude in the native PS I complex corresponds to the dipole with the negative charge located between F_A and F_B rather than on F_B itself. Based on the analysis of kinetics of $P700^+$ dark relaxation, the microscopic equilibrium constants between F_X and F_A as well as between F_A and F_B were recently estimated as 70 and 0.5–1.15, respectively (V.P. Shinkarev, I.R. Vassiliev and J.H. Golbeck, in preparation). Based on the known X-ray structure of PS I complex [11], the sum of projections of the center-to-center vectors from P700 to F_X to the membrane normal is equal to 33 Å, the projection for the $F_X \rightarrow F_A$ vector is 14 Å, while that for the $F_X \rightarrow F_B$ vector is 20 Å. We can recalculate the photovoltage amplitudes as normalized to the amplitude of the P700 to F_X electron transfer derived in the presence of dithionite. This will yield values of 1, 0.41 and 0.19 relative units for the $P700 \rightarrow F_X$, $F_X \rightarrow F_B$ and $F_X \rightarrow F_A$ components of $\Delta\Psi$, respectively (see Tables 1 and 2). Note that in the recent paper by Diaz-Quintana et al. [6], the corresponding $\Delta\Psi$ values were estimated as 1, 0.24 and 0.23 relative units, respectively. Thus the contribution of $\Delta\Psi$ component ascribed to $F_X \rightarrow F_A$ electron transfer is close to our value, while that for $F_X \rightarrow F_B$ is significantly lower. The reason for this discrepancy is not clear; however, there are differences in the PS I preparations, in the technique used to measure the electrogenic changes, and in the criterion used to normalize the $\Delta\Psi$.

The ratio between the dielectric $\varepsilon_{XB}/\varepsilon_{PX}$ is equal to 1.47 (see Table 1), while that for electron transfer from F_X to F_A and from P700 to F_X constants corresponding to electron transfer from F_X to F_B and from P700 to F_X ($\varepsilon_{XA}/\varepsilon_{PX}$) is 2.19 (Table 2). The lower $\varepsilon_{XB}/\varepsilon_{PX}$ value for the whole F_X-F_B region compared to $\varepsilon_{XA}/\varepsilon_{PX}$ for the F_X-F_A region assumes that the average effective dielectric constant value in the F_A-F_B region is lower relative to the F_X-F_A region. This result seems to be somewhat surprising, since it is not in line with the general three-phase model for the membrane proteins [17]. This model is mainly based on the comparison of the relative magnitudes of the electrogenic steps [18] and the distances between the corresponding cofactors in *Rhodopseudomonas viridis* reaction centers [19]. Accordingly, the redox centers more remote from the hydrophobic inner part of membrane protein are located in the protein region with the dielectric constant similar or higher to that of the inner part of the membrane. There are several notable exceptions to this general rule. For instance, the primary (Q_A) and the secondary (Q_B) quinone acceptors in the photosynthetic bacterial reaction centers are located at the same distance from the border of the protein dielectric [20,21]. However, Q_B is surrounded by more charged amino acid residues and water molecules than Q_A, which leads to a higher dielectric constant in its vicinity compared to Q_A [22,23]. The substantially higher effective dielectric constants were suggested in the vicinity of the redox cofactors of the functional branch than that for the non-functional branch of *Rhodobacter sphaeroides* reaction centers [24]. Taking into account these considerations, one may speculate that the observed decrease of the effective dielectric constant in the F_A-F_B region compared to the F_X-F_A region can be due to a more polar surrounding of the F_X-proximal F_A compared to the F_X-distal F_B cluster. Note also that the effective dielectric constant values are usually considered under static conditions where the variations of the electric field proceeds so slowly that protein polarization modes have enough time to respond to the changes of the field. Due to a wide range of atom and group mobilities in proteins, there exists a wide range of dielectric relaxation times, making the effective static constant dependent on the characteristic time of the process [25].

Our data therefore indicate that the voltage changes on the reducing side of PS I are related to electron transfer between F_X and F_A as well as between F_A and F_B. Based on the electrogenic nature of the latter reaction in PS I complexes, we conclude that F_B rather than F_A is the acceptor distal to F_X.

Acknowledgements: The authors thank Drs. Yean-Sung Jung and Fan Yang for isolation of PS I complexes. The work was supported by grants from the Civilian Research and Development Foundation (CRDF, RB1-214), from the Russian Foundation for Basic Research (97-04-50179), from the President of the Russian Federation Council for Grant Proposals (96-15-97043) and from the US National Science Foundation (MCB-969617a).

References

[1] Brettel, K. (1997) Biochim. Biophys. Acta 1318, 322–373.
[2] Sakurai, H., Inoue, K., Fujii, T. and Mathis, P. (1991) Photosynth. Res. 27, 65–71.
[3] He, W.Z. and Malkin, R. (1994) Photosynth. Res. 41, 381–388.
[4] Jung, Y.-S., Yu, L. and Golbeck, J.H. (1995) Photosynth. Res. 46, 249–255.
[5] Vassiliev, I.R., Jung, Y.-S., Yang, F. and Golbeck, J.H. (1998) Biophys. J. 74, 2029–2035.
[6] Diaz-Quintana, A., Leibl, W., Bottin, H. and Sétif, P. (1998) Biochemistry 37, 3429–3439.
[7] Leibl, W., Toupance, B. and Breton, J. (1995) Biochemistry 34, 10237–10244.
[8] Sigfridsson, K., Hansson, O. and Brzezinski, P. (1995) Proc. Natl. Acad. Sci. USA 92, 3458–3462.
[9] Mamedov, M.D., Gadjieva, R.M., Gourovskaya, K.N., Drachev, L.A. and Semenov, A.Yu. (1996) J. Bioenerg. Biomembr. 28, 517–522.
[10] Vos, M.H. and van Gorkom, H.J. (1990) Biophys. J. 58, 1547–1555.
[11] Schubert, W.-D., Klukas, O., Krauss, N., Saenger, W., Fromme, P. and Witt, H.T. (1997) J. Mol. Biol. 272, 741–769.
[12] Golbeck, J.H. (1995) in: CRC Handbook of Organic Photochemistry and Photobiology (Song, P.S. and Horspool, W.M., Eds.), pp. 1407–1419, CRC Press, Boca Raton, FL.
[13] Gourovskaya, K.N., Mamedov, M.D., Vassiliev, I.R., Golbeck, J.H. and Semenov, A.Yu. (1997) FEBS Lett. 414, 193–196.
[14] Vassiliev, I.R., Jung, Y.-S., Mamedov, M.D., Semenov, A.Yu. and Golbeck, J.H. (1997) Biophys. J. 72, 301–315.
[15] Brettel, K. and Golbeck, J.H. (1995) Photosynth. Res. 45, 183–193.
[16] Bentrop, D., Bertini, I., Luchinat, C., Nitschke, W. and Mühlenhoff, U. (1997) Biochemistry 36, 13929–13937.
[17] Cherepanov, D.A. and Krishtalik, L.I. (1990) Bioelectrochem. Bioenerg. 24, 113–127.
[18] Dracheva, S.M., Drachev, L.A., Konstantinov, A.A., Semenov, A.Yu., Skulachev, V.P., Arutjunjan, A.M., Shuvalov, V.A. and Zaberezhnaya, S.M. (1988) Eur. J. Biochem. 174, 253–264.
[19] Deisenhofer, J., Epp, O., Miki, K., Huber, R. and Michel, H. (1985) Nature 318, 618–624.
[20] Allen, J.P., Feher, G., Yeates, T.O., Komiya, H. and Rees, D.C. (1988) Proc. Natl. Acad. Sci. USA 85, 8487–8491.

[21] Okamura, M.Y. and Feher, G. (1992) Annu. Rev. Biochem. 61, 861–896.
[22] Ermler, U., Fritzsch, G., Buchanan, S.K. and Michel, H. (1994) Structure 2, 925–936.
[23] Stowell, M.H.B., McPhillips, T.M., Rees, D.C., Soltis, S.M., Abresch, E. and Feher, G. (1997) Science 276, 812–816.
[24] Steffen, M.A., Lao, K. and Boxer, S.G. (1994) Science 264, 810–816.
[25] Soriano, G.M., Cramer, W.A. and Krishtalik, L.I. (1997) Biophys. J. 73, 3265–3276.